A LETTERS JOURNAL EXPLORING THE FRONTIERS OF PHYSICS

OFFPRINT

Noise correlations controlled by dressed suppression and enhancement

HUAYAN LAN, IRFAN AHMED, HANG WANG, YIHENG YANG, HAIJUN TANG, YIQI ZHANG and YANPENG ZHANG

EPL, **115** (2016) 33001

A Letters Journal Exploring the Frontiers of Physics

AN INVITATION TO SUBMIT YOUR WORK

epljournal.org

The Editorial Board invites you to submit your letters to EPL

EPL is a leading international journal publishing original, innovative Letters in all areas of physics, ranging from condensed matter topics and interdisciplinary research to astrophysics, geophysics, plasma and fusion sciences, including those with application potential.

The high profile of the journal combined with the excellent scientific quality of the articles ensures that EPL is an essential resource for its worldwide audience. EPL offers authors global visibility and a great opportunity to share their work with others across the whole of the physics community.

Run by active scientists, for scientists

EPL is reviewed by scientists for scientists, to serve and support the international scientific community. The Editorial Board is a team of active research scientists with an expert understanding of the needs of both authors and researchers.

OVER
568,000
full text downloads in 2015

18 DAYS
average accept to online publication in 2015

20,300
citations in 2015

"We greatly appreciate the efficient, professional and rapid processing of our paper by your team."

Cong Lin
Shanghai University

Six good reasons to publish with EPL

We want to work with you to gain recognition for your research through worldwide visibility and high citations. As an EPL author, you will benefit from:

1. **Quality** – The 60+ Co-editors, who are experts in their field, oversee the entire peer-review process, from selection of the referees to making all final acceptance decisions.
2. **Convenience** – Easy to access compilations of recent articles in specific narrow fields available on the website.
3. **Speed of processing** – We aim to provide you with a quick and efficient service; the median time from submission to online publication is under 100 days.
4. **High visibility** – Strong promotion and visibility through material available at over 300 events annually, distributed via e-mail, and targeted mailshot newsletters.
5. **International reach** – Over 3200 institutions have access to EPL, enabling your work to be read by your peers in 100 countries.
6. **Open access** – Articles are offered open access for a one-off author payment; green open access on all others with a 12-month embargo.

Details on preparing, submitting and tracking the progress of your manuscript from submission to acceptance are available on the EPL submission website **epletters.net**.

If you would like further information about our author service or EPL in general, please visit **epljournal.org** or e-mail us at **info@epljournal.org**.

EPL is published in partnership with:

European Physical Society | Società Italiana di Fisica | EDP Sciences | IOP Publishing

A Letters Journal Exploring the Frontiers of Physics

August 2016

EPL, **115** (2016) 33001 www.epljournal.org
doi: 10.1209/0295-5075/115/33001

Noise correlations controlled by dressed suppression and enhancement

Huayan Lan[1,2(a)], Irfan Ahmed[1,3(a)], Hang Wang[1], Yiheng Yang[1], Haijun Tang[1], Yiqi Zhang[1] and Yanpeng Zhang[1(b)]

[1] *Key Laboratory for Physical Electronics and Devices of the Ministry of Education & Shaanxi Key Lab of Information Photonic Technique, Xi'an Jiaotong University - Xi'an 710049, China*
[2] *Yunnan Open Key Lab of Mechanics, Pu'er University - Pu'er 665000, China*
[3] *Electrical Engineering Department, Sukkur Institute of Business Administration - Air port Road, Sukkur 65200, Pakistan*

received 13 July 2016; accepted in final form 9 August 2016
published online 9 September 2016

PACS 32.50.+d – Fluorescence, phosphorescence (including quenching)
PACS 42.50.Gy – Effects of atomic coherence on propagation, absorption, and amplification of light; electromagnetically induced transparency and absorption
PACS 42.70.Mp – Nonlinear optical crystals

Abstract – The intensity noise correlations between anti-Stokes and Stokes fields, generated from spontaneous parametric four-wave mixing (SP-FWM) process have been investigated in a ladder-type three-level system of sodium atomic vapor. By introduction of an external dressing field, the strengthened (weakened) correlations are obtained under enhancement (suppression) condition of SP-FWM. Besides, sharp correlations have been obtained as attributed to a pair of non-classical beams generated from amplified spontaneous emission.

Introduction. – In recent years, the generations of a correlated photon pair and entangled photon sources have been extensively studied in atomic vapor as well as in crystal systems. Simultaneously, the correlated photon pair has been reported by Lukin *et al.* [1] and Kimble's group [2] experimentally. The $\chi^{(3)}$ processes in the multi-level atomic system, including stimulated Raman scattering [3–5] and multi-wave mixing via atomic coherence, play vital roles in producing correlated and entangled photons [6–9]. Moreover, the intensity noise correlations have been widely studied under electromagnetically induced transparency [10] with magnetic field [11]. Besides, the processes of atomic optical parametric oscillations in nonlinear crystal have also been reported [12]. Specially, the correlations between Stokes and anti-Stokes photons emitted from rubidium atoms with a short time delay have been measured [7]. It has also been shown that the correlations occur due to a four-wave mixing (FWM) process in cold atoms [13].

In this paper, through the SP-FWM process, Stokes and anti-Stokes two output weak fields are generated in a configuration of "double-Λ" level system (utilizing two hyperfine levels of sodium ground state) with a strong pumping field. Simultaneously, the fluorescence (FL) signals are also generated from the spontaneous emission of photons through the multi-nonlinear process. The intensity noise correlations between Stokes and anti-Stokes fields are studied experimentally and theoretically by changing the frequency detuning of the pumping field and seeding a new beam. Specifically, the correlations can be weakened/strengthened by introducing external dressing fields. Moreover, the variations of correlations are studied by increasing the power of a single dressing field as well as of multiple dressing fields. Finally, the correlation between Stokes and anti-Stokes fields generated by amplified spontaneous emission (ASE) is also studied.

Experimental setup and basic theory. – The experiments are performed in a three-level atomic system of sodium as depicted in fig. 1(a), where three energy levels are labeled as $3S_{1/2}$ ($|0\rangle$, $F = 1$; $|1\rangle$, $F = 2$), $3P_{1/2}(|2\rangle)$ and $4D_{3/2}$ ($|3\rangle$). Here, the FWM ($\boldsymbol{E}_{\rm F}$) process occurs in the cascade-type level subsystem ($|0\rangle$-$|1\rangle$-$|2\rangle$) involving $\boldsymbol{E}_1$, $\boldsymbol{E}_2$ and $\boldsymbol{E}_2'$ beams. $\boldsymbol{E}_{\rm F}$ propagates in opposite direction of $\boldsymbol{k}_2'$ and satisfies the phase-matching condition

(a) These authors contributed equally to this work.
(b) E-mail: ypzhang@mail.xjtu.edu.cn

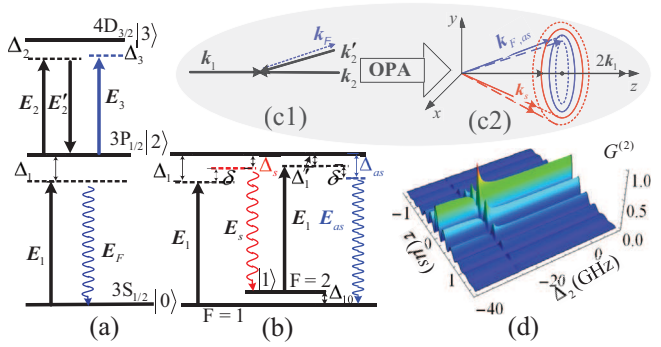

Fig. 1: (Color online) (a) A ladder-type level atomic system to generate $\boldsymbol{E}_{\rm F}$. (b) Double-Λ configuration for SP-FWM with laser coupling configuration to generate $\boldsymbol{E}_{\rm s}$ and $\boldsymbol{E}_{\rm as}$. (c) The schematic diagram of a FWM optical parametric amplifier (OPA) process with seeding $\boldsymbol{E}_{\rm F}$ into the $\boldsymbol{E}_{\rm as}$ channel. (d) Simulation of $G^{(2)}_{\rm as\text{-}s}$ *vs.* τ and Δ_2 with partial suppression/enhancement condition.

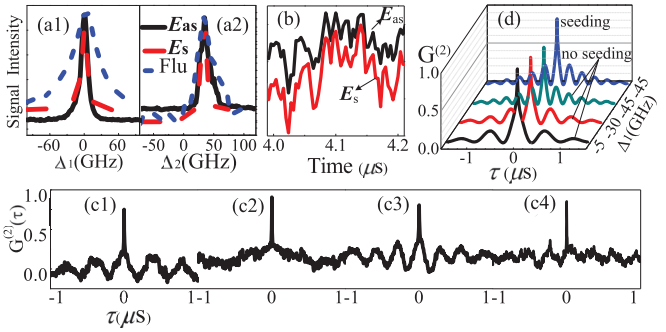

Fig. 2: (Color online) (a) Evolutions of $\boldsymbol{E}_{\rm as}$ (solid curve), $\boldsymbol{E}_{\rm s}$ (dashed curve) and FL (short-dashed curve) *vs.* Δ_1 (a1) and Δ_2 (a2). (b) Time domain wave forms of $\boldsymbol{E}_{\rm as}$ and $\boldsymbol{E}_{\rm s}$ at $\Delta_1 = -30\,$GHz with opening $\boldsymbol{E}_1$ only. (c) $G^{(2)}_{\rm as\text{-}s}(\tau)$ *vs.* τ at $\Delta_1 = -5\,$GHz (c1), $-30\,$GHz (c2), $-45\,$GHz (c3) with no seeding, while (c4) shows seeding of $\boldsymbol{E}_{\rm F}$ at $\Delta_2 = -\Delta_1$. (d) Simulations of $G^{(2)}_{\rm as\text{-}s}(\tau)$ under the same conditions as defined in (c).

$\boldsymbol{k}_{\rm F} = \boldsymbol{k}_1 + \boldsymbol{k}_2 - \boldsymbol{k}'_2$ as shown in fig. 1(c1). Meanwhile, an effective SP-FWM is produced in a "double-Λ" configuration shown in fig. 1(b). This process also satisfies the phase-matching condition $\boldsymbol{k}_{\rm s} + \boldsymbol{k}_{\rm as} = 2\boldsymbol{k}_1$ and the energy conservation $\omega_{\rm s} + \omega_{\rm as} = 2\omega_1$, where $\omega_{\rm s} = \varpi_{\rm s} + \delta$ and $\omega_{\rm as} = \varpi_{\rm as} - \delta$; here δ is the line width and $\varpi_{\rm s,as}$ is the center frequency of $\boldsymbol{E}_{\rm s,as}$. When $\boldsymbol{E}_{\rm F}$ is injected into the $\boldsymbol{E}_{\rm as}$ channel, the $\boldsymbol{E}_{\rm s}$ and $\boldsymbol{E}_{\rm as}$ signals can be amplified as shown in fig. 1(c2). This injection is used to configure the linear phase-insensitive OPA [14].

In the current experiment, all participating beams come from three near-transform-limited dye lasers pumped by a Nd:YAG laser (10 Hz repetition rate, 5 ns pulse width and $0.04\,{\rm cm}^{-1}$ line width). Therefore, the frequencies ω_i of the pumping field ($\boldsymbol{E}_1$) and driving fields ($\boldsymbol{E}_{2,3}$ and $\boldsymbol{E}'_2$) are associated with these lasers whose frequency detunings and Rabi frequencies are defined as $\Delta_i = \Omega_{mn} - \omega_i$ $(i = 1, 2, 3)$ and $G_i = \mu_{mn}E_i/\hbar$ ($G'_{\rm i} = \mu_{mn}E'_i/\hbar$), respectively. Here Ω_{mn} and μ_{mn} denote the transition frequency and dipole moment between $|m\rangle$ and $|n\rangle$ with the transverse relaxation rate Γ_{mn}, and E_i the electric-field intensity. These output signals $\boldsymbol{E}_{\rm F}$, $\boldsymbol{E}_{\rm s}$, $\boldsymbol{E}_{\rm as}$ including fluorescence (FL) are captured by photomultiplier tubes.

Now, we present a brief theory of SP-FWM. By opening the strong pumping field $\boldsymbol{E}_1$, $\boldsymbol{E}_{\rm s}$ and $\boldsymbol{E}_{\rm as}$ are emitted, forming a conical emission [15] as shown in fig. 1(c2). The Hamiltonian of such a system is defined as $H = (\hat{a}^\dagger\hat{b}^\dagger + \hat{a}\hat{b})g/v$, where $\hat{a}^\dagger$, $\hat{b}^\dagger$ $(\hat{a}, \hat{b})$ are the creation (annihilation) operators acting on the electromagnetic excitation of the $\boldsymbol{E}_{\rm s}$ and $\boldsymbol{E}_{\rm as}$, respectively. v is the group velocity of the light in the nonlinear medium, and $g = |-i\omega_{\rm as,s}\chi^{(3)}_{\rm as,s}\mathbf{E}_1\mathbf{E}_1/2c|$ is the parameter of the amplifier relying on the nonlinearity $\chi^{(3)}$ and the amplitude of pumping field. $\chi^{(3)}_{\rm as,s}$ is proportional to the density matrix elements of $\boldsymbol{E}_{\rm as/s}$. The density matrix elements of the generated Stokes and anti-Stokes fields with the opening of a stronger dressing field $\boldsymbol{E}_2$ can be written as

$$\rho^{(3)}_{21({\rm s})} = -iG^*_{\rm as}G_1^2/ [(d_{21} + |G_2|^2/d_{31})d_{01}(d'_{21} + |G_2|^2/d'_{31})], \quad (1a)$$

$$\rho^{(3)}_{20({\rm as})} = -iG^*_{\rm s}G_1^2/ [(d_{20} + |G_2|^2/d_{30})d_{10}(d'_{20} + |G_2|^2/d'_{30})] \quad (1b)$$

through Liouville's pathways $\rho^{(0)}_{11} \xrightarrow{\omega_1} \rho^{(1)}_{21} \xrightarrow{-\omega_{\rm as}} \rho^{(3)}_{01} \xrightarrow{\omega_1} \rho^{(3)}_{21({\rm s})}$ and $\rho^{(0)}_{00} \xrightarrow{\omega_1} \rho^{(1)}_{20} \xrightarrow{-\omega_{\rm s}} \rho^{(3)}_{10} \xrightarrow{\omega_1} \rho^{(3)}_{20({\rm as})}$, respectively, where $d_{21} = \Gamma_{21} + i\Delta'_1$, $d'_{21} = \Gamma_{21} + i(\Delta_1 - \delta)$, $d_{01} = \Gamma_{01} - i\delta$, $d_{20} = \Gamma_{20} + i\Delta_1$, $d_{10} = \Gamma_{10} + i\delta$, $d'_{20} = \Gamma_{20} + i(\Delta'_1 + \delta)$, $d_{31} = \Gamma_{31} + i(\Delta'_1 + \Delta_2)$, $d_{30} = \Gamma_{30} + i(\Delta_1 + \Delta_2)$, $d'_{31} = \Gamma_{31} + i(\Delta_1 - \delta + \Delta_2)$, $d'_{30} = \Gamma_{30} + i(\Delta'_1 + \delta + \Delta_2)$.

When $\boldsymbol{E}_2$ and $\boldsymbol{E}'_2$ are open, the FWM signal can be obtained with spatial configuration (fig. 2(c1)). Via the Liouville pathway $\rho^{(0)}_{00} \xrightarrow{\omega_1} \rho^{(1)}_{20} \xrightarrow{\omega_2} \rho^{(2)}_{30} \xrightarrow{-\omega_2} \rho^{(3)}_{20({\rm F})}$, the corresponding density matrix element can be written as

$$\rho^{(3)}_{20({\rm F})} = -iG_1G_2G'^*_2/(d_{20}^2 d_{30}). \quad (2)$$

As per the spatial configuration depicted in fig. 1(c), $\boldsymbol{E}_{\rm F}$ is injected into the $\boldsymbol{E}_{\rm as}$ channel. Such parametric amplification process can be described by the perturbation chain $\rho^{(0)}_{00} \xrightarrow{\omega_1} \rho^{(1)}_{20} \xrightarrow{-\omega_{\rm F}} \rho^{(2)}_{10} \xrightarrow{\omega_1} \rho^{(3)}_{20({\rm as})}$ with the phase-matching condition $\boldsymbol{k}_{\rm as} = 2\boldsymbol{k}_1 - \boldsymbol{k}_{\rm s}$, and the density matrix element (eq. (2)) is modified as

$$\rho'^{(3)}_{21({\rm s})} = -iG^*_{\rm F}G_1^2/[(d_{21} + |G_2|^2/d_{31})d_{01}(d'_{21} + |G_2|^2/d'_{31})], \quad (3)$$

where $G_{\rm F} \propto \sqrt{2/\varepsilon_0 c\hbar^2}N\mu_{10}^2\rho^{(3)}_{\rm F}$.

When $\boldsymbol{E}_{\rm s}$ and $\boldsymbol{E}_{\rm as}$ propagate through nonlinear medium, they evolve under the Hamiltonian of the system, whose photon numbers can be defined as

$$\langle\hat{a}^\dagger\hat{a}\rangle = \left\{\cosh\left[2t\sqrt{G}\cos\varphi\right] - \cos\left[2t\sqrt{G}\sin\varphi\right]\right\} \times \left(1 + |\alpha|^2\right)g_{\rm s}/(2g_{\rm as}), \quad (4a)$$

$$\langle \hat{b}^\dagger \hat{b} \rangle = \left\{ \cosh\left[2t\sqrt{G}\cos\varphi\right] - \cos\left[2t\sqrt{G}\sin\varphi\right] \right\} \frac{g_{\rm as}}{2g_{\rm s}} + \frac{1}{2}\left\{ \cosh\left[2t\sqrt{G}\cos\varphi\right] + \cos\left[2t\sqrt{G}\sin\varphi\right] \right\} |\alpha|^2 , \quad (4b)$$

where $G = g_{\rm s}g_{\rm as}$, $\varphi = (\varphi_{\rm s} + \varphi_{\rm as})/2$, $\varphi_{\rm s}$ and $\varphi_{\rm as}$ are the phase angles of $\boldsymbol{E}_{\rm s}$ and $\boldsymbol{E}_{\rm as}$. Here, $\alpha = 0$ without seeding beam; when FWM is seeded $\alpha = \pi r^2 \varepsilon_0 ch|G_{\rm F}|^2/(2\mu_{10}^2\omega_{\rm F})$, where r is the waist radius.

The intensity noise correlation function $G^{(2)}(\tau)$ between Stokes and anti-Stokes fields can be calculated by [13]

$$G^{(2)}_{\text{as-s}}(\tau) = \langle \delta I_{\rm as}(t)\delta I_{\rm s}(t+\tau)\rangle \,/\, \sqrt{\langle[\delta I_{\rm as}(t)]^2\rangle \langle[\delta I_{\rm s}(t+\tau]^2\rangle} \quad (5)$$

The intensities of $\boldsymbol{E}_{\rm s}$ and $\boldsymbol{E}_{\rm as}$ are proportional to the numbers of photons $\langle \hat{a}^\dagger \hat{a}\rangle$ and $\langle \hat{b}^\dagger \hat{b}\rangle$, respectively. So the correlation function $G^{(2)}_{\text{as-s}}(\tau)$ between $\boldsymbol{E}_{\rm s}$ and $\boldsymbol{E}_{\rm as}$ without seeding beam can be expressed as

$$G^{(2)}_{\text{as-s}}(\tau) = A\,|A_1|^2\,R/\sqrt{BCDE}, \quad (6)$$

where $A = [e^{-2\Gamma_+|\tau|} + e^{-2\Gamma_-|\tau|} - 2\cos(\Omega_{\rm e}|\tau|)) \times e^{-(\Gamma_+ + \Gamma_-)|\tau|}]$, $R = |R_{\rm s}R_{\rm as}\boldsymbol{E}_{\rm s}\boldsymbol{E}_{\rm as}|^2$, $A_1 = A_2 N \times (\mu_{10}\mu_{20}E_1)^2\varpi_{\rm as}L/(2c\varepsilon_0\hbar^3)$, and $\Omega_{\rm e}$ are the Rabi oscillations. Here, $\Gamma_+ = \Gamma_{10}$, $\Gamma_- = \Gamma_{20}$, $\Omega_{\rm e} = |\Delta_1|$, $A_2 = 1/d_{20}$ are without dressing fields, whereas $\Gamma_\pm = [(\Gamma_{30}+\Gamma_{20})/2] \pm [\Delta_2(\Gamma_{20}-\Gamma_{30})/(4\Omega_{\rm e}^2 + 8\Gamma_{20}\Gamma_{30})^{1/2}]$, $\Omega_{\rm e} = (4|G_2|^2 + \Delta_2^2)^{1/2}$ and $A_2 = 1/(d_{20} + |G_2|^2/d_{30})$ are with dressing field $\boldsymbol{E}_2$. B, C, D and E are constants, which are not related with the delay time τ [16]. The three-dimensional simulation of $G^{(2)}_{\text{as-s}}$ *vs.* Δ_2 and τ at fixed Δ_1 is shown in fig. 1(d). We can see that $G^{(2)}_{\text{as-s}}$ is modulated to a smaller value at the suppression point and to a larger one at the enhancement point.

If $\boldsymbol{E}_{\rm F}$ is seeded into anti-Stokes channel, the correlation function $G^{(2)}_{\text{as-s}}(\tau)$ can be rewritten as

$$G^{(2)}_{\text{as-s}}(\tau) = [A\,|A_1|^2\,R(1+|\alpha|^2) - DC\,|\alpha|^2]/\sqrt{BCDE}. \quad (7)$$

For the sake of comparison, the results of eq. (7) are larger than those of eq. (6) due to $A|A_1|^2R - DC > 0$.

Experimental results and discussions. – Figure 2(a1) shows the spectrum of $\boldsymbol{E}_{\rm as}$, $\boldsymbol{E}_{\rm s}$ and FL *vs.* Δ_1 by opening pumping field $\boldsymbol{E}_1$ only. $\boldsymbol{E}_{\rm s}$ and $\boldsymbol{E}_{\rm as}$ signals show the emission peak determined by eq. (1) while having no dressing effect from $\boldsymbol{E}_2(|G_2|^2/d_{31}$ and $|G_2|^2/d_{30})$. FL can be described by the density matrix element $\rho_{22}^{(2)} = |G_1|^2/(\Gamma_{22}d_{20}) + \text{H.c.}$ Figure 2(b) shows the typical wave forms of $\boldsymbol{E}_{\rm as}$ and $\boldsymbol{E}_{\rm s}$ in the time domain at $\Delta_1 = -30\,\text{GHz}$. The correlation function $G^{(2)}_{\text{as-s}}(\tau)$ between Stokes and anti-Stokes output is from eq. (5), which is calculated at $\Delta_1 = -5\,\text{GHz}$ (fig. 2(c1)), $-30\,\text{GHz}$ (fig. 2(c2)) and $-45\,\text{GHz}$ (fig. 2(c3)). While the peaks equal to $G^{(2)}_{\text{as-s}}(\tau)$ at delay time $\tau = 0$ have positive amplitudes equal to 0.752, 0.888 and 0.768, respectively. As $\boldsymbol{E}_{\rm as}$ and $\boldsymbol{E}_{\rm s}$ are coherent photon pairs, they both increase or decrease synchronously. Comparing the values of $G^{(2)}_{\text{as-s}}(0)$ at different frequency detunings, we found that the correlation in the off-resonance region is larger than that in the near-resonance one as signals are strongly absorbed under the resonance region. So the correlation is slightly destroyed. The correlation $G^{(2)}_{\text{as-s}}(0)$ decreases with increasing $|\Delta_1|$ in the off-resonant region due to the reduction in the generation of SP-FWM. The theoretical simulations show similar results, but the correlation is largest at $\Delta_1 = 0$ as absorptions of the signals are not considered theoretically. It is notable that the Rabbi oscillation period ($T = 2\pi/\Omega_{\rm e}$) decreases from figs. 2(c1) to (c3) when $|\Delta_1|$ becomes large. Besides, a sharp peak is superimposed on the spectrum of the correlation $G^{(2)}_{\text{as-s}}(\tau)$ at $\tau = 0$, as shown in figs. 2(c1)–(c3). This is due to the correlation of the other pair of SP-FWM generated by ASE with broad line width [17]. Theoretically, the correlation function can be written as eq. (6) but the parameter A is expressed as $A = [e^{-(2\Gamma_+ + \zeta)|\tau|} + e^{-(2\Gamma_- + \zeta)|\tau|} - 2\cos(\Omega_{\rm e}|\tau|)e^{-(\Gamma_+ + \Gamma_- + \zeta)|\tau|}]$ with the line width ζ of ASE and $\zeta \gg \Gamma$. So the correlation peak is very sharp and the Rabbi oscillation is weakened and it even disappears.

As other two fields $\boldsymbol{E}_2$ and $\boldsymbol{E}_2'$ are opened, the output $\boldsymbol{E}_{\rm F}$ is injected into the anti-Stoke channel, as shown in fig. 1(c2). The amplified output signals $\boldsymbol{E}_{\rm as}$ (solid curve) and $\boldsymbol{E}_{\rm s}$ (dashed curve) accompanied by two-photon FL (short-dashed curve) satisfying two-photon resonance $\Delta_1 + \Delta_2 = 0$ are shown in fig. 2(a2) with $\Delta_1 = -45\,\text{GHz}$. The correlation $G^{(2)}_{\text{as-s}}(0) = 0.827$ in fig. 2(c4) is larger than that in fig. 2(c3). In order to explain the increased intensity noise correlation, the output signals $\boldsymbol{E}_{\rm as}$ and $\boldsymbol{E}_{\rm s}$ should be considered. From eq. (4), $\boldsymbol{E}_{\rm as}$ and $\boldsymbol{E}_{\rm s}$ are gained from parametric amplification. Hence the fluctuations of SP-FWM as well as their consistency become remarkable. For the amplified SP-FWM, $G^{(2)}_{\text{as-s}}(\tau)$ increases as the numerator in eq. (7) is larger with seeding of $\boldsymbol{E}_{\rm F}$ (described as $|\alpha|^2$) than that without seeding in eq. (6).

Now, we investigate $G^{(2)}_{\text{as-s}}(\tau)$ under enhancement and suppression conditions of SP-FWM in fig. 3. Figure 3(a) shows the intensities of $\boldsymbol{E}_{\rm as}$ (solid curve), $\boldsymbol{E}_{\rm s}$ (dashed curve) and FL (short-dashed curve) *vs.* Δ_2 with opening single dressing field $\boldsymbol{E}_2$ and setting Δ_1 at $-5\,\text{GHz}$, $-30\,\text{GHz}$ and $-45\,\text{GHz}$. The SP-FWM ($\boldsymbol{E}_{\rm as}$ and $\boldsymbol{E}_{\rm s}$) signal varies from pure suppression (fig. 3(a1)), to partial enhancement/suppression (fig. 3(a2)) and then to pure enhancement (fig. 3(a3)), but the FL signal shows a moving two-photon emission peak described by the term d_{30} in $\rho_{33}^{(4)} = |G_1|^2|G_2|^2/(\Gamma_{33}d_{20}d_{30}d_{32}) + \text{H.c.}$ According to eq. (1), the corresponding enhancement and suppression conditions of $\boldsymbol{E}_{\rm as}$ ($\boldsymbol{E}_{\rm s}$) are $\Delta_1 + \Delta_2/2 \pm (\Delta_2^2 + 4G_2^2)^{1/2}/2 = 0$ ($\Delta_1' + \Delta_2/2 \pm (\Delta_2^2 + 4G_2^2)^{1/2}/2 = 0$) and $\Delta_1 + \Delta_2 = 0$ ($\Delta_1' + \Delta_2 = 0$), respectively. The theoretical simulations of $\boldsymbol{E}_{\rm as}$ are shown in fig. 3(b) with the same conditions

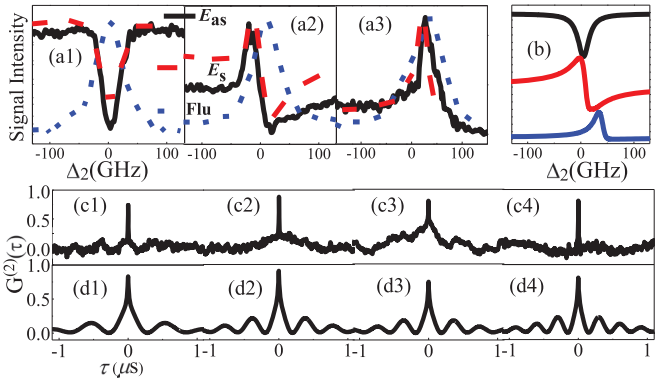

Fig. 3: (Color online) (a) Measured signals of $\boldsymbol{E}_{\rm as}$ (solid curve), $\boldsymbol{E}_{\rm s}$ (dashed curve) and FL (short-dashed curve) *vs.* Δ_2 by opening $\boldsymbol{E}_1$ and $\boldsymbol{E}_2$ ($P_2 = 200\,\mu$W) with the same detunings as those defined in figs. 2(c1)–(c3). (b) Simulations of $\boldsymbol{E}_{\rm as}$ from top to bottom with the same conditions as defined in (a1)–(a3). (c) $G^{(2)}_{\rm as\text{-}s}(\tau)$ with pure suppression (c1), partial enhancement (c2), partial suppression (c3) and pure enhancement conditions (c4). (d) Simulations of $G^{(2)}_{\rm as\text{-}s}(\tau)$ corresponding to (c).

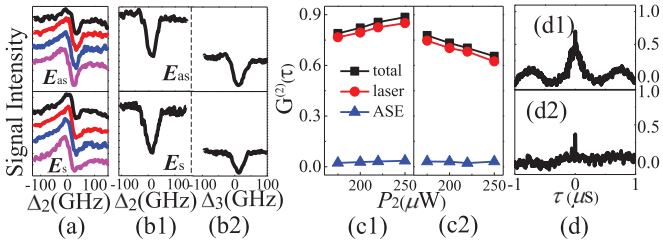

Fig. 4: (Color online) (a) Measurement of $\boldsymbol{E}_{\rm as}$ and $\boldsymbol{E}_{\rm s}$ *vs.* Δ_2 by increasing the power of $\boldsymbol{E}_2$ from the top curve to the bottom and blocking $\boldsymbol{E}_2'$ and $\boldsymbol{E}_3$ at $\Delta_1 = -28\,$GHz. (b) Intensities of SP-FWM with single dressing field $\boldsymbol{E}_2$ (b1) and double dressing fields $\boldsymbol{E}_2$ and $\boldsymbol{E}_3$ at $\Delta_1 = -3.5\,$GHz (b2). (c) Dependence of $G^{(3)}_{\rm as\text{-}s}(0)$ at partial enhancement (c1) and suppression points (c2). (d) $G^{(2)}_{\rm as\text{-}s}(\tau)$ with (1) single and (2) double dressing effect.

defined in fig. 3(a). Using eq. (6), the correlations are calculated at pure suppression, partial enhancement, partial suppression and pure enhancement points, as shown in figs. 3(c1)–(c4), respectively. In order to investigate the variations of $G^{(2)}_{\rm as\text{-}s}(\tau)$, the calculated results in fig. 3(c) are compared with those in figs. 2(c1)–(c3). The correlation $G^{(2)}_{\rm as\text{-}s}(0) = 0.739$ in fig. 3(c1) with external dressing field $\boldsymbol{E}_2$ is smaller than that in fig. 2(c1) without $\boldsymbol{E}_2$ having the same frequency detuning $\Delta_1 = -5\,$GHz. The reason is that $\boldsymbol{E}_{\rm as}$ and $\boldsymbol{E}_{\rm s}$ are being suppressed by the dressing field $\boldsymbol{E}_2$. Therefore, $G^{(2)}_{\rm as\text{-}s}(0)$ has also a smaller value in fig. 3(c3) at the partial suppression point when compared with that in fig. 2(c2). However, $G^{(2)}_{\rm as\text{-}s}(0) = 0.883$ at the partial enhancement point in fig. 3(c2) is larger than that in fig. 2(c2), and a similar situation in $G^{(2)}_{\rm as\text{-}s}(0)$ at the enhancement point with $\Delta_1 = -45\,$GHz is shown in fig. 3(c4) when compared with that in fig. 2(c3). The reason is that $\boldsymbol{E}_{\rm as}$ and $\boldsymbol{E}_{\rm s}$ are enhanced under the enhancement condition.

Based on the above comparative analysis, one can say that $G^{(2)}_{\rm as\text{-}s}(\tau)$ can be controlled by the dressed enhancement/suppression of the external field. Theoretically, the amplitude of $G^{(2)}_{\rm as\text{-}s}(\tau)$ depends on the coefficient A_1 in eq. (8). If the dressing field $\boldsymbol{E}_2$ is open, the dressing effect determined by $|G_2|^2/d_{30}$ in A_2 will act on the correlation function (eq. (6)). Thus, $G^{(2)}_{\rm as\text{-}s}(\tau)$ with the enhancement condition is larger than that without dressing field; on the contrary, an opposite result may be obtained under the suppression condition. The simulations in fig. 3(d) are in good agreement with the experimental results of fig. 3(c).

Figure 4(a) shows the spectral intensities of $\boldsymbol{E}_{\rm as}$ and $\boldsymbol{E}_{\rm s}$ *vs.* Δ_2 with setting power of $\boldsymbol{E}_2$ at $175\,\mu$W, $200\,\mu$W, $220\,\mu$W and $250\,\mu$W from top to bottom, respectively. The partial enhancement/suppression of $\boldsymbol{E}_{\rm as}$ and $\boldsymbol{E}_{\rm s}$ becomes more obvious as increasing power of $\boldsymbol{E}_2$ due to the enhanced dressing effect determined by $|G_2|^2/d_{30}$ and $|G_2|^2/d_{31}$ in eq. (1). Correspondingly, the dependence of the calculated $G^{(2)}_{\rm as\text{-}s}(0)$ at partial enhancement and partial suppression points are shown in figs. 4(c1) and (c2), respectively. $G^{(2)}_{\rm as\text{-}s}(0)$ (squares) in fig. 4(c1) gradually increases with the increase in power of $\boldsymbol{E}_2$ from $175\,\mu$W to $250\,\mu$W, which is mainly caused by enhanced nonlinear coherence under the enhancement condition. But $G^{(2)}_{\rm as\text{-}s}(0)$ (triangles) generated by ASE is nearly invariable. Therefore, an opposite variation of $G^{(2)}_{\rm as\text{-}s}(0)$ appears at the partial suppression point due to the gradually weakened nonlinear coherence, as shown in fig. 4(c2).

In fig. 4(b1), a suppression dip appears in $\boldsymbol{E}_{\rm as}$ and $\boldsymbol{E}_{\rm s}$ signals with single dressing field $\boldsymbol{E}_2$ only and scanning it for the same reason as in fig. 3(a1). When we set $\boldsymbol{E}_{\rm as}$ and $\boldsymbol{E}_{\rm s}$ at the suppression dip in fig. 4(b1) and scan the other dressing field $\boldsymbol{E}_3$, the signals are suppressed more severely as shown in fig. 4(b2) due to the double dressing effect of $\boldsymbol{E}_2$ and $\boldsymbol{E}_3$. The correlation $G^{(2)}_{\rm as\text{-}s}(0) = 0.688$ in fig. 4(d1) is larger than that in fig. 4(d2) ($G^{(2)}_{\rm as\text{-}s}(0) = 0.369$). It is because SP-FWM suffers stronger dressing effects with double dressing fields than with single dressing field. Hence the suppression effect of SP-FWM is stronger under double dressing. Theoretically, the dressing effect is enhanced when $\boldsymbol{E}_3$ is open, the dressing term $|G_3|^2/[\Gamma_{30} + i(\Delta_1 + \Delta_3)]$ should be added into the term A_2 of eq. (6) except for $|G_2|^2/d_{30}$. Hence $G^{(2)}_{\rm as\text{-}s}(\tau)$ decreases further when compared with the single dressing field. Based on the analysis of the experimental results, the dressing effect on $G^{(2)}_{\rm as\text{-}s}(\tau)$ with increasing power of the dressing field is analogous to increasing the numbers of dressing fields. So the enhanced or suppressed $G^{(2)}_{\rm as\text{-}s}(\tau)$ at the enhancement or suppression point can be controlled in these two manners.

Summary. – In summary, we have experimentally observed and theoretically demonstrated the simultaneous

generations of $\boldsymbol{E}_{\rm as}$ and $\boldsymbol{E}_{\rm s}$ as accompanied by FL signals in sodium atomic vapors. Moreover, the control of the intensity noise correlations between $\boldsymbol{E}_{\rm as}$ and $\boldsymbol{E}_{\rm s}$ is attributed to frequency detuning of pumping field, seeding beam and the dressing effect of the external field. Specifically, the correlation values become smaller with larger frequency detuning, while correlations become higher as $\boldsymbol{E}_{\rm as}$ and $\boldsymbol{E}_{\rm s}$ are amplified with the seeding beam at larger frequency detuning. Under the influence of the external dressing field, the correlation is reduced under the suppression condition but strengthened under the enhancement condition when the external dressing field is involved. Besides, the dressing effect on the correlation with increasing power of the dressing field is analogous to increasing the number of dressing fields. Nevertheless, the correlation between $\boldsymbol{E}_{\rm as}$ and $\boldsymbol{E}_{\rm s}$ generated by ASE is not currently controlled by the dressing effect. These studies can be used for information communication.

* * *

This work was supported by the 973 Program (2012CB921804), NSFC (11474228, 61308015, 11265012), NSFC of Shaanxi Province (2014JZ020, 2014JQ8341).

REFERENCES

[1] van der Wal C. H., Eisaman M. D., André A., Walsworth R. L., Phillips D. F., Zibrov A. S. and Lukin M. D., *Science*, **301** (2003) 196.

[2] Kuzmich A., Bowen W. P., Boozer A. D., Boca A., Chou C. W., Duan L. M. and Kimble H. J., *Nature*, **423** (2003) 731.

[3] Golub I., *Opt. Lett.*, **20** (1995) 1847.

[4] Niggl L. and Maier M., *Opt. Lett.*, **22** (1997) 910.

[5] Klewitz S., Leiderer P., Herminghaus S. and Sogomonian S., *Opt. Lett.*, **21** (1996) 248.

[6] Thompson J. K., Simon J., Loh H. and Vuletić V., *Science*, **313** (2006) 74.

[7] Balić V., Braje D. A., Kolchin P., Yin G. Y. and Harris S. E., *Phys. Rev. Lett.*, **94** (2005) 183601.

[8] Yan H., Zhang S. C., Chen J. F., Loy M. M. T., Wong G. K. L. and Du S. W., *Phys. Rev. Lett.*, **106** (2011) 033601.

[9] Boyer V., Marino A. M., Pooser R. C. and Lett P. D., *Science*, **321** (2008) 544.

[10] Harris S. E., *Phys. Today*, **50**, issue No. 7 (1997) 36.

[11] Sautenkov V. A., Rostovtsev Y. V. and Scully M. O., *Phys. Rev. A*, **72** (2005) 065801.

[12] Okuma J., Hayashi N., Fujisawa A., Mitsunaga M. and Harada K., *Opt. Lett.*, **34** (2009) 698.

[13] Braje D. A., Balić V., Goda S., Yin G. Y. and Harris S. E., *Phys. Rev. Lett.*, **93** (2004) 183601.

[14] Pooser R. C., Marino A. M., Boyer V., Jones K. M. and Lett P. D., *Phys. Rev. Lett.*, **103** (2009) 010501.

[15] Motomura K., Tsukamoto M., Wakiyama A., Harada K. and Mitsunaga M., *Phys. Rev. A*, **71** (2005) 043817.

[16] Chen H. X., Qin M. Z., Zhang Y. Q., Zhang X., Wen F., Wen J. M. and Zhang Y. P., *Laser Phys. Lett.*, **11** (2014) 045201.

[17] Zheng H. B., Zhang X., Zhang Z. Y., Tian Y. L., Chen H. X., Li C. B. and Zhang Y. P., *Sci. Rep.*, **3** (2013) 1885.